Journal of Coastal and Marine Engineering
Volume 1 • Number 1• June 2018

Numerical Study of the Effect of Current Velocity on Power Production by a Horizontal Axis Marine Current Turbine and Feasibility of Using It in the Straint Of Hormuz

Amir Honaryar[1*], Mahmoud Ghiasi[2*]

1) Faculty of Maritime Technology, Amirkabir University of Technology, Tehran, Iran, Yarehonar@aut.ac.ir
2) Faculty of Maritime Technology, Amirkabir University of Technology, Tehran, Iran, Mghiasi@aut.ac.ir

Abstract: The effect of current velocity on power production by a Horizontal Axis Marine Current Turbine (HAMCT) has been investigated. In this paper, a two-step procedure was used for numerical analysis of the turbine. In the first step, Blade Element Momentum Theory (BEMT) was used to reach an initial configuration for the blades of turbine. Chord and twist distributions along the blade length, and hydrodynamic torque produced by HAMCT were estimated using this theory. Then in the second step, a numerical method based on Computational Fluid Dynamics (CFD) was used to achieve a better understanding of the turbine performance and fluid flow characteristics around the blades. Finally, feasibility of using the HAMCT in the Strait of Hormuz was studied. The CFD simulations provided the flow field within the computational domain. Spatial integration of the pressure distribution around the blades yields hydrodynamic torque generated by the HAMCT. The results have also provided the variation of rotor torque with the tidal current velocity. Findings showed that increase in the tidal current velocity to a little more than 2 m/s, increases the torque as the square of the velocity. However, increasing the velocity beyond 2 m/s doesn't change the torque. In other words, torque remains almost constant because the rotor speed is constant and equal to 11.5 rpm. Finally, it was concluded that by installing a marine power plant which consists of an array of 10 HMCT systems in the Qeshm channel, 10 MW power can be generated.

Keywords: Numerical Study, Boundary Element Momentum Theory (BEMT), Turbine, Computational Fluid Dynamics (CFD)

1. Introduction

World energy consumption has increased by sixty percent for thirty years (1980-2010) and it reached about 16000 GW in 2010 [1]. According to increasing global population growth, this demand will continue in the future.

As shown in Figure 1, fossil fuels such as Oil, Coal and Natural Gas have played the most important role in the world energy consumption thus far. However, fossil fuels have been associated with many disadvantages. In other words, due to the rate of increase in pollutants and greenhouse gas emissions, the need for renewable energy has increased in the world. Considerable portion of this energy can be extracted from the sea. Marine renewable energy can be divided into several types, including wave energy, tidal energy, ocean thermal energy, ocean current energy and salinity gradient energy. The tidal energy is also divided into tidal potential energy and tidal kinetic energy.

Due to its special geographical position and climate conditions, there is a good potential for exploitation of marine renewable energy in Iran. This country has a marine boundary of about 2700 km in its southern and northern regions, including 1259 km with the Persian Gulf, 784 km with the Gulf of Oman, and 657 km with the Caspian Sea [3]. Thus, the need for further research on marine renewable energy resources and their extraction sites in Iran has increased more than before.

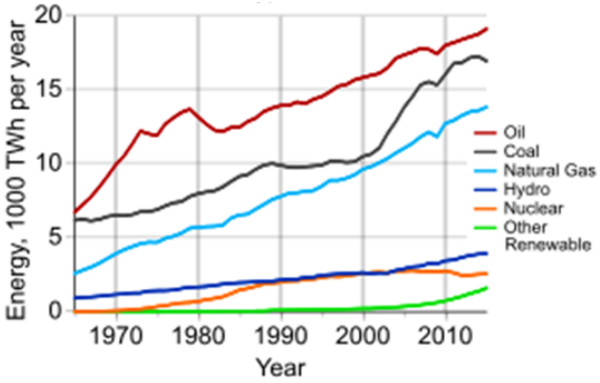

Figure 1. World energy consumption[2].

Marine currents can be divided into two categories, ocean and tidal. The latter has a greater potential in Iran, especially in the Persian Gulf. Horizontal Axis Marine Current Turbine (HAMCT) is one of the most effective tools for the extraction of tidal energy [4]. This energy is one of the most available energies of seas around the world. Tidal energy is created by the gravitational forces of the sun and the moon and the rotational motion of the earth. Predictability is one of the advantages offered by this energy over wind energy and this is an appropriate factor for marine current turbine compared with wind turbine [5].

Given that HAMCT places within the flow of water, which is an incompressible flow, hydrodynamic analysis is required to evaluate its characteristics such as productivity and efficiency. Blade Element Momentum Theory

*Corresponding author.

(BEMT) and Computational Fluid Dynamics (CFD) are two hydrodynamic evaluation approaches which are used to analyze the marine turbines.

Blade element momentum theory that was developed initially for wind turbines is a combination of bladeelement and momentum theory. With this theory, turbine efficiency can be expressed in the form of thrust and torque coefficients. Among people who were working in this field, Goundar [6], and Batten [7] can be cited. In their numerical model, the effect of geometrical and physical parameters such as pitch angle, chord length, lift and drag coefficients were examined and the Bahaj's experimental data [8] were used to validate the numerical data. Walker [9] also in 2014 used blade element theory to study experimentally and numerically, the impact of marine current turbine blade roughness on its performance.

Numerical solutions of the Navier-Stokes equations for incompressible flow using Computational Fluid Dynamics (CFD) include detailed procedures for marine current turbine in hydrodynamic analysis. In 2014, Gunawan [10] investigated a three-blade turbine using CFD. In 2015, Zhang et al. [11] applied CFD to numerically evaluate the impact of waves on the horizontal axis marine current turbine efficiency. They simulated a two-blade marine turbine with a diameter of 12 m in confronting with a marine current with speed of 1.7 m/s. In the same year, Noruzi et al. [4] used numerical simulation to evaluate the performance of the HAMCT in the presence of gravity waves and results of CFD compared with BEMT. Given that the method based on CFD numerically solves fluid flow motion equations, it is more accurate than methods based on blade element momentum theory. However, computational fluid dynamics methods require heavy computational cost. Therefore, in the early design stages of the turbine, the BEMT can be used and basic geometric configurations and specifications can be estimated and in the next stage, CFD can be applied to check the performance and behavior of the flow around the blades.

In this study, the potential of Iran as a marine country for tidal current energy extraction was investigated and the Persian Gulf and Strait of Hormuz in particular with respect to certain geographic locations were examined. Also, according to the appropriate position in the Strait of Hormuz, Qeshm channel was studied thoroughly. In this paper, a two-step procedure is used for numerical analysis of the turbine. In the first step, Blade Element Momentum Theory (BEMT) is used to reach an initial configuration for the blades of turbine. Chord and twist distributions along the blade length, and hydrodynamic torque produced by HAMCT are estimated using this theory. Then in the second step, a numerical method based on Computational Fluid Dynamics (CFD) was used to achieve a better understanding of the turbine performance and fluid flow characteristics around the blades.

2. Tidal Energy

Among renewable energies, energies in the seas and oceans have attracted much attention, because there is a significant portion of the energy in various forms in the seas, such as wave energy, tidal energy, thermal energy and current energy. Tidal energy is one of the most accessible energies in the sea. The most notable advantage over other renewable energies such as wind energy is that it is predictable.

Tide phenomenon is caused by gravitational force between the earth, sun and moon, and the moon plays a greater role in this phenomenon. Generally, tidal energy has been divided into two categories: potential energy of the water level difference and tidal current kinetic energy. Marine turbines are essentially similar to wind turbines, but due to the much more density of water than air, the marine current turbines can be used at low speeds of current. To produce equal power, marine turbines need lesser diameter than the wind turbines. Figure 2 shows a comparison between marine and wind turbines.

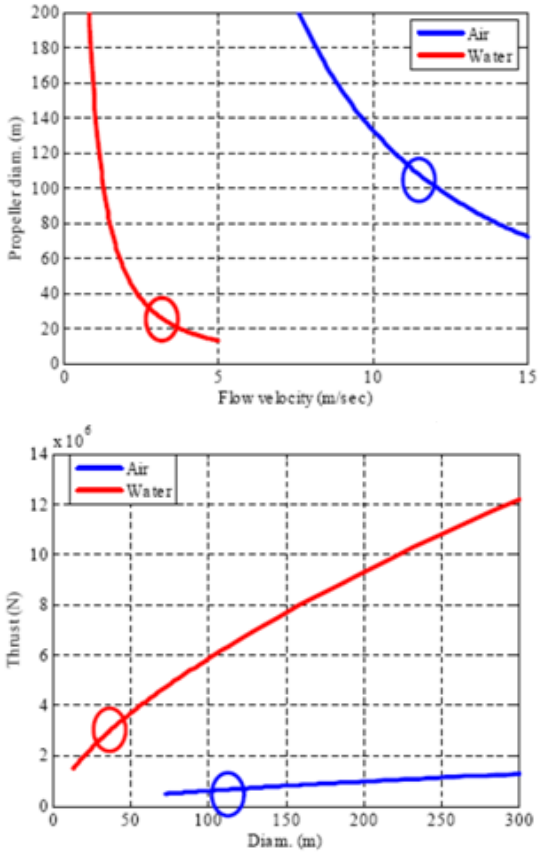

Figure 2. Comparison between marine and wind turbines: Required propeller diameter (Up) and Thrust versus diameter (Down) for a 5MW turbine[12].

2.1. Marine Current Turbine

Marine current power converters are divided into three main categories: 1) horizontal axis turbine, 2) vertical axis turbine and 3) oscillating hydrofoil. Horizontal axis marine current turbine is the most appropriate marine turbine which is widely used [4]. Figure 3 shows a horizontal axis marine current turbine which is brought to the surface for inspection. As previously noted, predictability is one of the benefits of tidal current energy and also is one of the advantages of marine turbine when compared to wind turbine [5].

Figure 3. Horizontal axis marine current turbine [13].

2.2. Tidal Current Energy Potentials in Iran

According to its position, between the seas in Iran, the Persian Gulf is the best for tidal current energy extraction. It is 1000 km long, 350 km wide with an average depth of 40 m [14]. As shown in Figure 4, the current speed exceeds 1 m/s in the Strait of Hormuz and in some areas, it reaches 2 m/s. In addition to appropriate areas in terms of tidal current speed, Qeshm, Hengam and Tonb-e Bozorg Islands and Bandarabbas can be noted. In these areas, the current speed is between 1 to 1.5 m/s [15]. Among these, a region in Qeshm channel with a width of 2600 m and the maximum depth of 29 m that is shown in Figure 5 is very suitable for exploitation of tidal kinetic energy. The tidal water-level in this region varies between 3-3.5 m leading to a tidal current velocity of about 3 m/s[16].

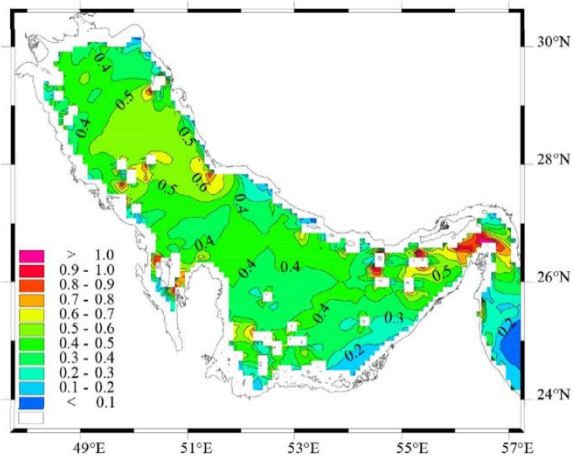

Figure 4. Tidal current velocity distribution in the Persian Gulf [13].

3. Turbine Configuration

As previously mentioned, the blade element momentum theory (BEMT) and computational fluid dynamics (CFD) are two methods for analyzing the marine current turbines. BEMT may be used in the early design stages to estimate the geometrical parameters such as chord length and pitch angle distributions along the blade length. This theory combines momentum and blade element theories to describe the hydrodynamic behavior of turbine blade. Hydrodynamic thrust and torque of the turbine blade can be obtained using BEMT as follows:

$$dT = 3dF_a = 3\left(dF_L \cos\varphi + dF_D \sin\varphi\right) = \frac{3}{2}\rho v_{rel}^2 .c.\left(C_L \cos\varphi + C_D \sin\varphi\right)dr \quad (1)$$

$$dM = 3rdF_u = 3r.\left(dF_L \sin\varphi - dF_D \cos\varphi\right) = \frac{3}{2}\rho v_{rel}^2 .c.\left(C_L \sin\varphi - C_D \cos\varphi\right).rdr \quad (2)$$

Where dF_a and dF_u are horizontal and vertical force components on blade element at radius r. dF_L and dF_D are local lift and drag forces, C_L and C_D are their coefficients, respectively. c is the chord length at r, v_{rel} relative velocity, φ flow angle, α angle of attack and β pitch angle, a axial and a' tangential induced velocity factor, and ω is the rotational speed of the turbine blade. These parameters are illustrated in Figure 6.

Figure 5. Qeshm channel in the Strait of Hormuz.

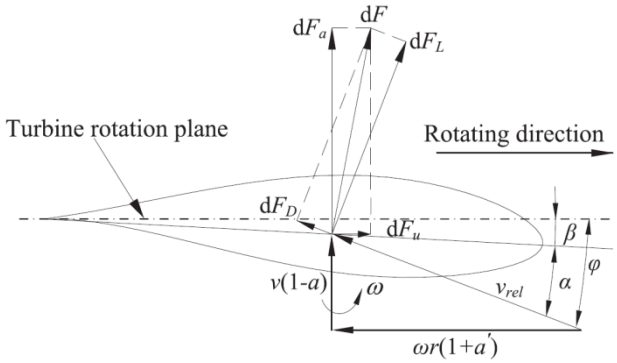

Figure 6. Force components on blade element.

As depicted in Figure 7, rotor diameter, tidal current conditions (velocity and direction), hydrofoil cross section, and hydrodynamic coefficients are input parameters for BEMT method. As output parameters of this method, number of blade, blade external shape and its geometric characteristics including chord and twist distribution along the radius of the blade are obtained. Of course, an optimization method such as genetic algorithm can be combined with BEMT to achieve optimal geometry. Then CFD may be used to analyze the fluid flow around the

blade more precisely and to obtain accurate torque produced by the marine current turbine.

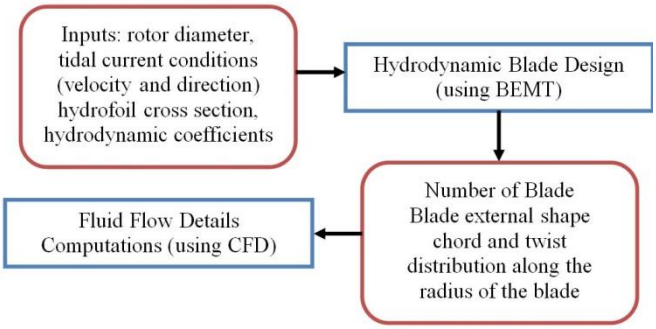

Figure 7. Hydrodynamic design process of Marine Current Turbine.

In this paper, the same geometry as geometry extracted by Bir et al. [17] for blade and its configuration is evaluated. The basic configuration and geometry for this turbine was obtained using numerical tool Harp_Opt which combines BEMT with genetic algorithm to provide optimal geometry characteristics of the turbine. Technical specifications of the HAMCT are shown in Table 1.

Table 1. Technical specifications of HAMCT.

Turbine Type	Horizontal Axis
No. Of Blades	2
Rotor diameter	20 m
Hub diameter	2 m
Rotor speed	11.5 rpm
Blade cross section	NACA 63$_1$-424

The geometric modeling of horizontal axis marine current turbine is depicted in Figure 8.

According to Equations (1) and (2), to calculate the thrust and torque using BEMT, it is necessary to obtain the lift and drag coefficients. Lift and drag coefficients versus angle of attacks are ploted in Figures 9 and 10, respectively for NACA63 series.

4. Numerical Analysis

Among the factors contributing to efficiency of marine current turbine, the current velocity, current angle of attack and geometry of turbine blades can be mentioned. In this paper, the effect of current velocity on power production by a horizontal axis marine current turbine was studied numerically.

4.1. Governing Equations

To study the efficiency of marine current turbine, it is necessary to obtain hydrodynamic torque which yields power produced by turbine. This torque can be calculated by velocity and pressure distribution. To obtain velocity and pressure distribution, governing equations for fluid flow i.e. mass conservation and Navier-Stokes equations are solved. By applying RANS method, these equations can be written as follows:

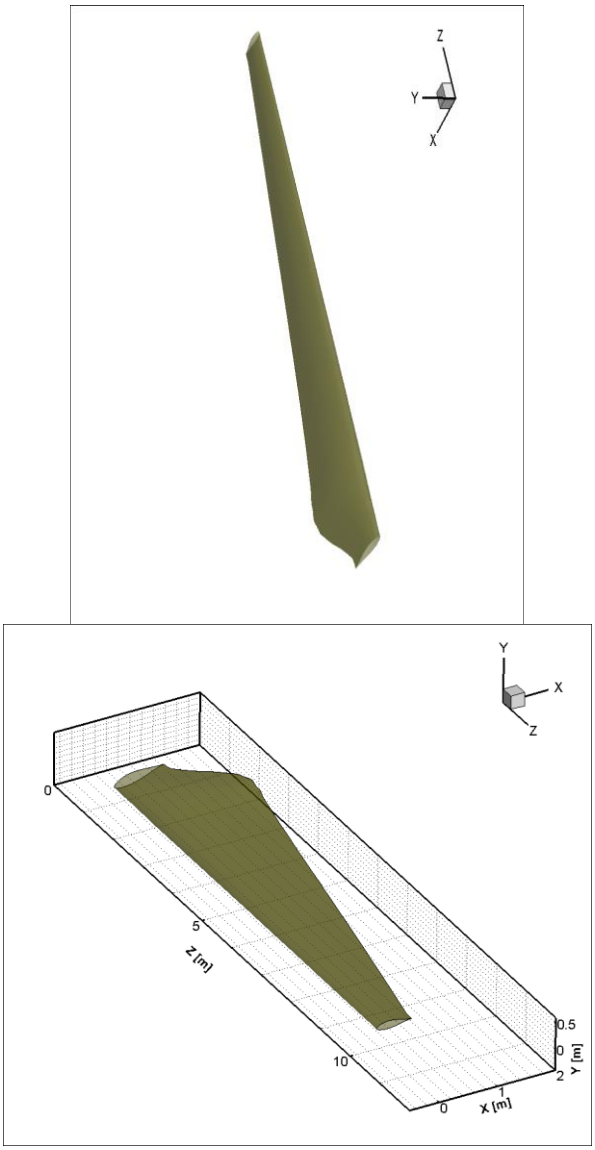

Figure 8. Geometric modeling of HAMCT blade.

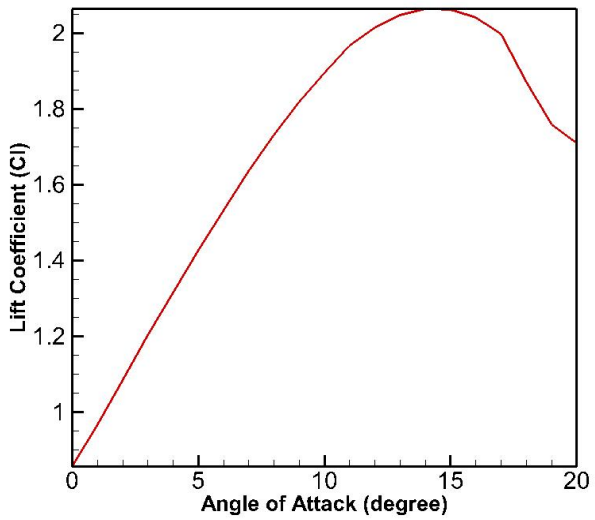

Figure 9. Lift coefficient versus angle of attack.

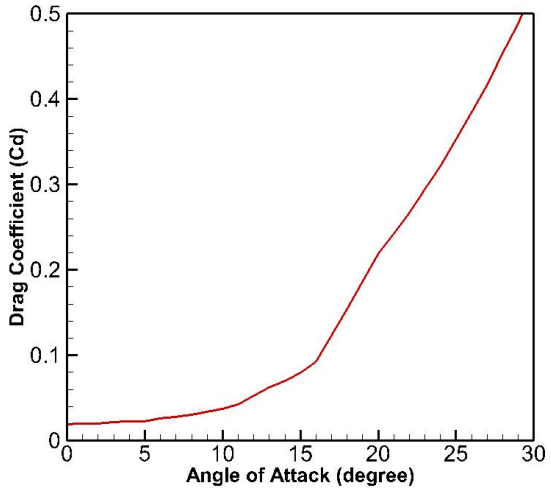

Figure 10. Drag coefficient versus angle of attack.

$$\frac{\partial \rho}{\partial t}+\frac{\partial}{\partial x_i}\left(\rho U_i\right)=0 \quad (3)$$

$$\frac{\partial \rho U_j}{\partial t}+\frac{\partial}{\partial x_i}\left(\rho U_j U_i\right)=-\frac{\partial P}{\partial x_j}+\frac{\partial}{\partial x_i}\left(\tau_{ji}-\rho u_j u_i\right)+S_M \quad (4)$$

where P is pressure and U is velocity vector.

4.2. Numerical Method

According to computational fluid dynamic (CFD), an element based finite volume code is used to solve RANS equations. Time derivative terms are discretized using the second order backward implicit scheme. This type of discretization is highly suitable for transient computations. Also, using a high resolution scheme which had second-order accuracy, the advection terms are discretized. Among turbulence models, (SST) $k-\omega$ was selected, where k and ω are turbulence kinetic energy and specific turbulence dissipation rate in transport equations, respectively.

This turbulence model solves two transport equations (5, 6) for k and ω.

$$\frac{\partial \rho k}{\partial t}+\nabla.\left(\rho k U\right)=\nabla\left(\gamma_k \nabla k\right)+G_k+Y_k \quad (5)$$

$$\frac{\partial\left(\rho\omega\right)}{\partial t}+\nabla\left(\rho\omega U\right)=\nabla\left(\gamma_\omega \nabla\omega\right)+G_\omega-Y_\omega+D_\omega \quad (6)$$

where Y_k and Y_ω represent the dissipation of k and ω, respectively and G_k and G_ω are the production of k and ω, respectively and Γ_k and Γ_ω are the effective diffusivity of k and ω, respectively. D_ω is the cross-diffusion term.

4.3. Solution Domain

To apply the finite volume code to turbine geometry, two types of domains which are stationary and rotating are created. The rotor is considered inside the rotating domain. Interfaces have been defined between the stationary and the rotating domains. As shown in Figure 10, the blade is placed in a cylindrical domain.

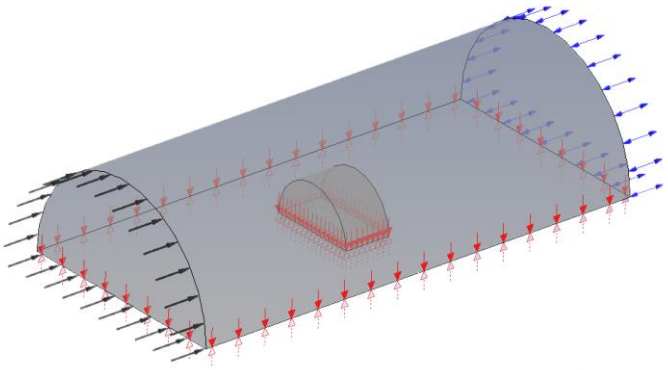

Figure 11. Computational domain for CFD analysis.

The blade is placed in a cylindrical domain. Because of symmetry, CFD simulations are applied for just one blade of the rotor that is modeled in a sector of 180°, instead of modeling the whole domain.

4.4. Boundary Conditions

The Dirichlet boundary condition is applied on the inlet boundary, in other words, the velocity of the flow in the inlet is defined. Static boundary condition and opening boundary condition are applied to outlet boundary for steady and transient solution, respectively. Turbine blade surface is modeled as a no slip wall boundary condition. Periodic condition is chosen for the sides boundaries to account for the rotational flow and General Geometry Interface (GGI) is applied for the interface between the inner and outer subdomains. Computational nodes and elements on the blade surface are illustrated in Figure 12.

4.5. Validation of the CFD Simulations

The error analysis has been examined from two aspects; one is the sensitivity of the numerical results to the grid and the discretization of the problem and the second is the verification of the results. Thickness of inflation layer, first layer thickness, and mesh quality are three of the most effective factors in the discretization of the problem which should be selected appropriately to minimize the computational error. The thickness of inflation layer should be chosen in such a way as to include the boundary layer. The thickness of the boundary layer can be estimated using Prandtl's relation for turbulent flow [18], $0.16L_S / \mathrm{Re}_{L_S}^{1/7}$ where L_S is the surface length including surface curvature and Re_{L_S} indicates Reynolds number based on L_S. Considering the fact that the first layer thickness Δy determines the non-dimensional wall distance, $y^+ = \rho u^* y_{wall} / \mu$ where u^* is friction velocity and y_{wall} represents wall distance, it may be used to

estimate the desired y^+ values. Using first layer thickness approximation for the flat plate, Δy is obtained from

$$\Delta y = l y^+ \sqrt{80}\,\mathrm{Re}^{-13/14} \tag{7}$$

where l is the length scale. The non-dimensional wall distance significantly depends on the selected turbulence model to calculate the Reynolds stress tensor. Considering the use of (SST) $k-\omega$ as a turbulent model in this study, the wall function approach is valid if $y^+ < 300$; however, it should be lower than 2 to take full advantage of the low Reynolds formulation.

Figure 12. Computational nodes and elements on the blade surface.

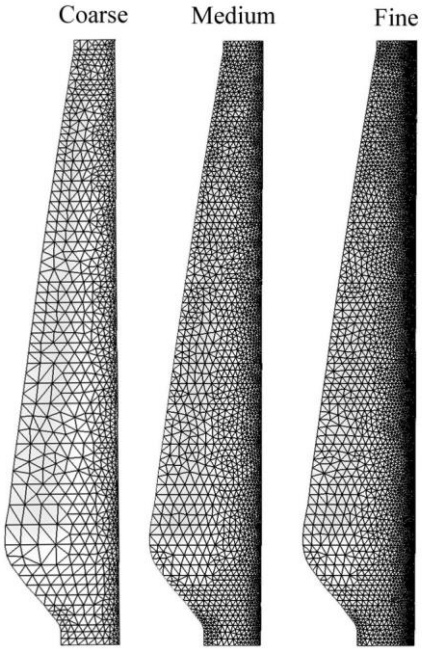

Figure 13. Element distribution on the blade for three 1.1, 2.4, and 3.3 mesh configuration named coarse, medium and fine, respectively.

In order to evaluate the mesh quality, mesh independence study is performed in such a way that the sensitivity of the results is compared with the number of elements for the four different mesh qualities. These four mesh configurations have 1.1, 2.4, 3.3, and 4 million elements, respectively. The elements on the blade for the first three configurations, named coarse, medium and fine, are depicted in Figure 13. As shown in this figure, the density of the elements, especially on the leading edge of the blade has increased from coarse to fine configuration, respectively.

To investigate the independence of the grid, the predicted results for torque generated by turbine are compared for four mesh configurations. The differences of the CFD results for torque produced by turbine from the finest 4 million elements mesh configuration versus number of elements are plotted in Figure 13. It is observed that the percentage difference from finest mesh for 1.1, 2.4, and 3.3, respectively are within23, 5, and 0.4%. Due to low and acceptable difference, for the remainder of the study, third mesh configuration with 3.3 million elements is chosen to save the computational time.

In order to verify the accuracy of the results, CFD predictions were compared with the results obtained by Bir et al. [17]. In this comparison, the geometry of the problem, turbulent model, and boundary conditions are the same in both methods, but the only difference is in solver and probably there is a slight difference in grid generation too. As will be described in the next section (Figure 15), the results are in reasonable agreement with the CFD predictions provided by Bir et al. [17]. It can be realized that as the current velocity increases, the difference increases and reaches its maximum value of 3.8% as the relative error, which may be due to the non-linearization of the relationships and using different solvers.

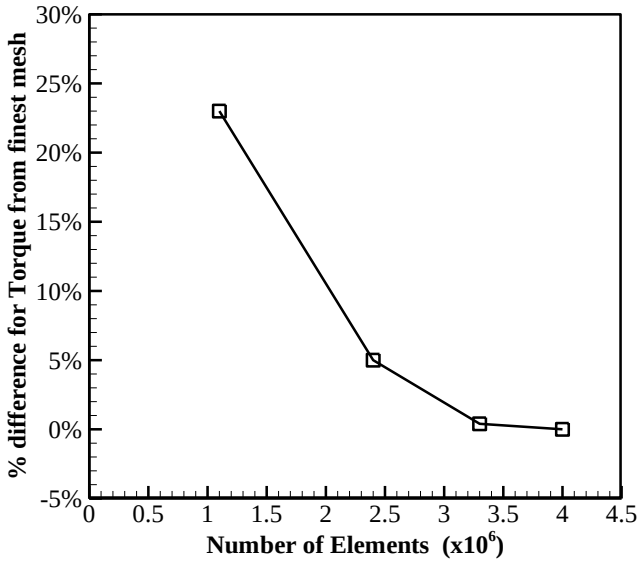

Figure 14. Percentage difference of the predicted torque produced by turbine from the finest 4 million elements mesh configuration versus number of elements .

5. Results and Discussion

The results are presented in two sections; the first part is devoted to the numerical results of the horizontal axis marine current turbine obtained from the computational fluid dynamics, and the second is devoted to the feasibility study of using this marine current turbine in Strait of Hormuz and Qeshm channel.

5.1. CFD Results

The CFD simulations provide the flow field within the computational domain. Finally, by solving RANS equations, the pressure and velocity fields were obtained numerically. Figure 15 shows the pressure distribution on the turbine blade.

By obtaining pressure distribution on the blade surface and integrating that over the blade surface area, the hydrodynamic thrust and torque can be calculated.

As shown in Figure 15, the pressure has high values on the leading edge over the blade radius. These high values are shown with red color. Also, as can be seen, the pressure falls on the tip region of the blade which is depicted with green or blue color. In this region, cavitation may occur especially when the current velocity increases and therefore considerations must be taken to prevent this phenomenon.

As mentioned earlier, spatial integration of the pressure distribution yields load distribution, specifically the torque generated by rotor as depicted in Figure 16. This figure shows the variation of rotor torque with the tidal current velocity. Also the results are validated with Bir et al. [17] work. As illustrated in Figure 16, when the tidal current velocity increases to a little more than 2 m/s, the torque goes up as the square of the velocity. But then with increasing velocity, torque remains almost constant because the rotor speed is constant and is equal to 11.5 rpm.

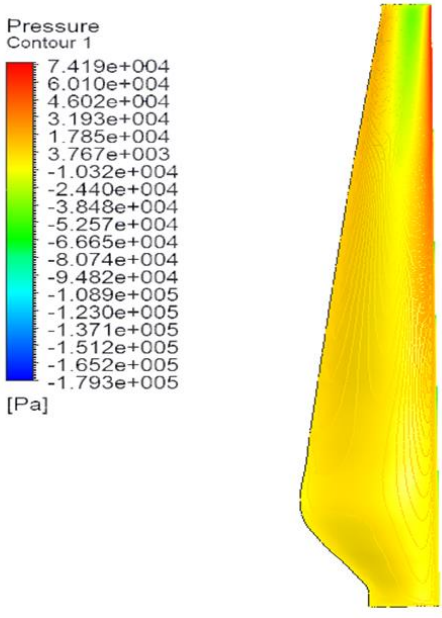

Figure 15. Pressure distribiution on the blade.

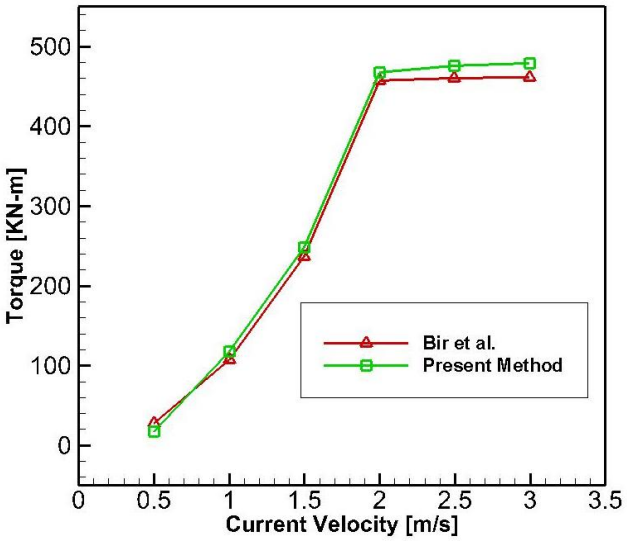

Figure 16. Generated torque versus current velocity.

5.2. Feasibility Study

As previously mentioned, an area in the Qeshm channel somewhere between Pohl and Laft ports is very suitable for tidal kinetic energy extraction, considering its tidal current velocity which reaches up to 3 m/s. Therefore, in the present study, a horizontal axis marine current turbine with specified geometry and configuration for application in this area was proposed.

In reaction to current-induced hydrodynamic forces, marine current turbine converts the kinetic energy of the tidal current into electrical energy using blades undergoing rotational motions. In comparison with vertical axis marine current turbine, the HAMCT axis is aligned with the dominant direction of the current, and this feature brings advantages for HAMCT. For example, from the perspective of power efficiency, HAMCT is better than VAMCT. However, power efficiency of HAMCT is so sensitive to the angle between turbine axis and current direction while power capturing capability of the VAMCT isn't. This feature causes the use of VAMCT in areas with bidirectional tidal currents. Therefore, since the current in Qeshm Strait is tidal and bidirectional, considerations should be given to apply HAMCT, in order to have more power efficiency, in Qeshm Strait. One solution for HAMCT is adopting the blades with bidirectional current in such a way that it doesn't need to be oriented based on one direction. In the present study, such a solution was used for geometry and configuration of turbine. Unsteadiness is another aspect of the tidal current in Qeshm Strait and should be considered in design process from the perspective of energy storage. Due to periodicity of the tidal phenomenon, the power produced by electric generators of the marine current turbines is highly oscillatory. To overcome this problem, a proper power storage system can be used. Therefore, the type of battery used as an energy storage system is effective. For example, to smooth the long-period power oscillations, high-energy batteries are advantageous.

Finally, it can be concluded that by installing this horizontal marine current turbine in Qeshm channel in the Strait of Hormuz, 1 MW power can be produced, and by using a marine power plant as shown in Figure 17 which consists of an array of 10 marine current turbine systems, this amount will increase to 10 MW.

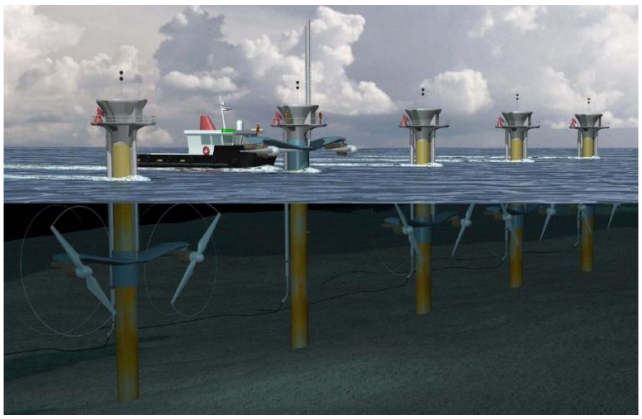

Figure 17.Marine power plant consists of an array of 10 marine current turbine systems proposed for use in the Strait of Hormuz (Qeshm Channel).

6. Conclusion

The effect of current velocity on power production by a Horizontal Axis Marine Current Turbine (HAMCT) was investigated. In this paper, a two-step procedure was used for numerical analysis of the turbine. In the first step, Blade Element Momentum Theory (BEMT) was used to reach an initial configuration for the blades of the turbine. Chord and twist distributions along the blade length, and hydrodynamic torque produced by HAMCT were estimated using this theory. Then in the second step, a numerical method based on Computational Fluid Dynamics (CFD) was used to achieve a better understanding of the turbine performance and fluid flow characteristics around the blades. Hydrodynamic thrust and torque were obtained from pressure distribution on the blade. The rotor torque was calculated versus tidal current velocity. Finally, feasibility of using the HAMCT in the Strait of Hormuz was studied. The CFD simulations provided the flow field within the computational domain. Spatial integration of the pressure distribution around the blades yielded hydrodynamic torque generated by the HAMCT. The results also provided the variation of rotor torque with the tidal current velocity. Findings showed that with increase in the tidal current velocity to a little more than 2 m/s, the torque goes up as the square of the velocity. But increasing velocity beyond 2 m/s doesn't change the torque. In other words, torque remains almost constant because the rotor speed is constant and is equal to 11.5 rpm. Finally, it was concluded that by installing a marine power plant which consists of an array of 10 HMCT systems in the Qeshm channel, 10 MW power can be generated.

7. References

[1]Zabihian, F. and Fung, A. S., "Review of marine renewable energies: Case study of Iran," *Renew. Sustain. Energy Rev.*, vol. 15, no. 5, pp. 2461–2474, 2011.

[2]"https://Our Finite World.com," 2013.

[3]Agency, N. G.-I., "Red Sea and the Persian," no. 866, 2011.

[4]Noruzi, R., Vahidzadeh, M., and Riasi, A., "Design, analysis and predicting hydrokinetic performance of a horizontal marine current axial turbine by consideration of turbine installation depth," *Ocean Eng.*, vol. 108, pp. 789–798, 2015.

[5]Zhou, Z., Benbouzid, M., Frédéric, J., Charpentier, Scuiller, F., and Tang, T., "A review of energy storage technologies for marine current energy systems," *Renewable and Sustainable Energy Reviews*, vol. 18. pp. 390–400, 2013.

[6]Goundar, J. N., Ahmed, M. R., and Lee, Y. H., "Numerical and experimental studies on hydrofoils for marine current turbines," *Renew. Energy*, vol. 42, pp. 173–179, 2012.

[7]Batten, W. M. J., Bahaj, S., Molland, F., and Chaplin, J. R., "The prediction of the hydrodynamic performance of marine current turbines," *Renew. Energy*, vol. 33, no. 5, pp. 1085–1096, 2008.

[8]Bahaj, S., Molland, F., Chaplin, J. R., and Batten, W. M. J., "Power and thrust measurements of marine current turbines under various hydrodynamic flow conditions in a cavitation tunnel and a towing tank," *Renew. Energy*, vol. 32, no. 3, pp. 407–426, 2007.

[9]Walker, J. M., Flack, K. A., Lust, E. E., Schultz, M. P., and Luznik, L., "Experimental and numerical studies of blade roughness and fouling on marine current turbine performance," *Renew. Energy*, vol. 66, pp. 257–267, 2014.

[10]Gunawan, B., Michelen, C., Neary, V., Coe, R., Johnson, E., Fontaine, A., Meyer, R. S., Straka, W., and Jonson, M., "Model validation using experimental measurements from the Garfield Thomas Water Tunnel at the Applied Research Laboratory (Arl) at Penn State University," pp. 1–4, 2014.

[11]Zhang, L., Wang, S. Q., Sheng, Q., Jing, F., and Ma, Y., "The effects of roll motion of the floating platform on hydrodynamics performance of horizontal-axis tidal current turbine," *J. Mar. Sci. Technol.*, vol. 74, pp. 1–11, 2016.

[12]Turnock, S. R., Nicholls-Lee, R., Wood, R. J. K., and Wharton, J. a., "Tidal turbines that survive?" University of Southampton, 2009.

[13]Li, Y., "On the definition of the power coefficient of tidal current turbines and efficiency of tidal current turbine farms," *Renew. Energy*, vol. 68, pp. 868–875, 2014.

[14]Pous, S., Carton, X., and Lazure, P., "A Process Study of the Tidal Circulation in the Persian Gulf," *Open J. Mar. Sci.*, vol. 2, no. 4, pp. 131–140, 2012.

[15]AGENCY, N. G.-I., "Red Sea and the Persian," *Natl. geospatial-intelligence agency*, vol. 172, no. 866, 2011.

[16]Soleimani, K., Ketabdari, M. J., and Khorasani, F., "Feasibility study on tidal and wave energy conversion in Iranian

seas," *Sustain. Energy Technol. Assessments*, vol. 11, pp. 77–86, 2015.

[17]Bir, G. S., Lawson, M. J., and Li, Y., "Structural design of a horizontal-axis tidal current turbine composite blade," in *ASME 30th International Conference on Ocean, Offshore, and Arctic Engineering*, 2011, no. October, p. 14.

[18]White, F. M., *Fluid Mechanics*, McGraw-Hil. New York, 2003.